Letter   Editors' Suggestion

Marangoni convection driven by temperature gradient near an isotropic-nematic phase transition point

Jun Yoshioka [*], Tasuku Sakikawa, Yuki Ito, and Koji Fukao
Department of Physical Sciences, Ritsumeikan University, 1-1-1 Noji-Higashi, Kusatsu, Shiga 525-5877, Japan

Marangoni flow driven by a temperature gradient was observed near the isotropic-nematic phase transition point. By applying the gradient to a liquid crystalline material in sandwich cells, it was possible to measure the flow field near the air interface using the photobleaching method. In the isotropic phase, the direction of the observed flow was opposite to that in the nematic phase. Moreover, when the measurement was performed in the coexistence state of these phases, the flow direction depended on the coating materials of the cell substrates. These singular flow properties are explained well by the singular changes in surface tension and the shape of the air interface near the transition point.

Phase transitions in fluid systems are often accompanied by flows. For example, in a liquid-gas transition, intense heat and material flows are often induced, as observed in the evaporation and boiling processes of working fluids in a heat pump and a steam engine [1], or in the Leidenfrost phenomenon with levitation and self-propulsion of liquid droplets [2–7]. It is well known that the evolution of flows is attributed to the singularity of physical properties, such as the existence of latent heat and drastic volume change at the phase transition point [8]. Moreover, evaporation often results in the appearance of a surface tension gradient such that the Marangoni flow is driven in the liquid-gas interface [9–13]. Characteristic material transportation phenomena resulting from this flow have been observed, known as "tears of wine" and "coffeering" effects [14–22]. The liquid-gas transition often results in singular flow phenomena owing to the singular properties at the phase transition point. Such a singularity should generally appear at the transition point.

In this study, the focus was on the Marangoni flow driven by a temperature gradient in a liquid crystalline system with an isotropic-nematic (I-N) phase transition. In typical liquids, the flow from the high- to low-temperature side of the surface has often been observed because the surface tension γ increases with a decrease in temperature T ($\partial \gamma / \partial T < 0$) [2,23–30]. However, this tendency has not necessarily been observed in materials with liquid crystalline phases. In the nematic (N) and smectic phases, both dependencies of $\partial \gamma / \partial T < 0$ and $\partial \gamma / \partial T > 0$ have often been reported, depending on the temperature and the materials [31–40]. In these liquid crystalline phases, the evolution of Marangoni flows under a temperature gradient has recently been observed [41–48]. Here, one may consider that the flow direction should be controlled by the T dependence of γ. This is supported by experimental results of Ref. [47] reported in 2019. It was observed that the direction

of the Marangoni flow in freely suspended smectic films under a temperature gradient depended on whether the material showed $\partial \gamma / \partial T < 0$ or $\partial \gamma / \partial T > 0$. The T dependence of γ, however, shows complex behavior near the I-N transition point. In addition to the drastic increase and decrease of γ, a discontinuous jump at the point has often been observed, depending on the materials [31–38]. It is quite natural to expect that this singularity in γ would strongly affect the Marangoni flow. Thus, in this study, the flow induced by the temperature gradient near the I-N phase transition point was observed and analyzed.

A calamitic liquid crystalline molecule of 7CB (LCC Co., Ltd.) was used, and, for the flow-field measurement with a photobleaching method, a fluorescence dye of C6-NBD ceramide (Cayman Chemical Co.) was added into 7CB at a weight ratio of 0.05%. The phase sequence of 7CB was N-41 °C-I. To apply a temperature gradient, 7CB was inserted into a sandwich cell made of copper foil spacers (50 μm thick) and cover glass substrates, as shown in Fig. 1(c). The substrates were coated with Al1254, JALS204 (Japan Synthetic Rubber Co., Ltd.), CYTOP (Asahi Glass Co., Ltd.) [49], or dimethyloctadecyl [3-(trimethoxysilyl)propyl] ammonium chloride (DMOAP, Sigma-Aldrich Co. LLC). The coating with Al1254 resulted in a planar anchoring, while a homeotropic anchoring was induced by JALS204, CYTOP, or DMOAP. After coating, the substrates with Al1254 were rubbed unidirectionally. Using a homemade temperature controller, the temperature gradient was applied to the sandwich cells, as shown in Fig. 1(a) (for more details, see a previous report of Ref. [43]). The flow field near the air interface in the sandwich cell was measured using the fluorescence photobleaching method described in Refs. [43,45,50]. The sample was bleached with a striped pattern using a photomask with a periodic array of slits. The flow velocity was obtained from the time evolution of the fluorescence microscope image after photobleaching. The temperature dependence of the surface tension of 7CB was measured using the method described in Refs. [40,51] (for more details, see Supplemental
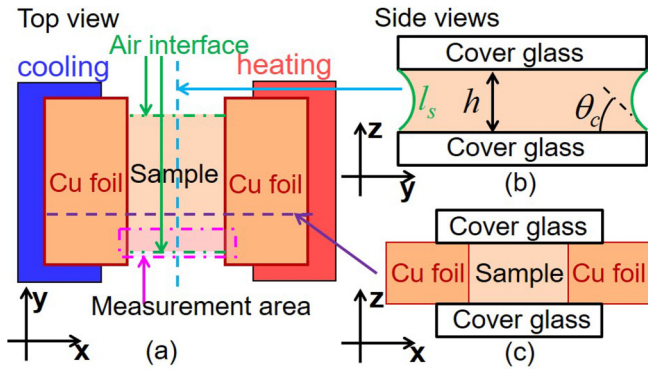
_____
[*]j-yoshi@fc.ritsumei.ac.jp

FIG. 1. Schematic illustration of the experimental setup in the flow-field measurement under temperature gradient. Cross-sectional views normal to z, x, and y axes are shown in (a)–(c), respectively. As shown in (a), the temperature gradient was applied by cooling and heating of the left and right copper foil spacers, respectively (for more details, see Ref. [43]). The flow field near the air interface was measured [the area enclosed by the pink rectangle in (a)]. In (b), the cell thickness h, contact angle θ_c, and length of the interface l_s are defined.

Material 1 [52]). Moreover, the contact angle [2] was measured in the sessile droplets of 7CB on cover glasses coated with Al1254, JALS204, CYTOP, and DMOAP.

First, the temperature dependence of the surface tension of 7CB was measured. In the N phase, the tension γ decreased with an increase in temperature T ($\partial\gamma/\partial T < 0$), while it showed a drastic increase just above the I-N transition point ($\partial\gamma/\partial T > 0$). In the I phase, the tendency of $\partial\gamma/\partial T > 0$ was observed in the temperature region from the transition point up to approximately 47 °C (for more details, see Supplemental Material 1 [52]). The inversion of the temperature dependence of the surface tension near the I-N transition point in 7CB has also been found by measurements using the pendant drop method in Ref. [35].

Next, the flow field near the air interface was measured under a temperature gradient using the experimental system illustrated in Fig. 1. In the measurement, the distribution of the flow velocity along the y axis (defined as the direction normal to that of the temperature gradient, as shown in Fig. 1) was obtained. In the N phase, the flow away from the interface was observed on the low-temperature side, and the flow toward the interface was on the high-temperature side, as shown in Fig. 2(a). In addition, the flow speed decayed with distance from the air interface. These results indicate the existence of a circulating flow localized near the interface, as shown in Fig. 2(c); thus, we should consider that the Marangoni flow from the high- to the low-temperature side is induced in the air interface in the N phase. However, in the I phase, a flow in the opposite direction was observed, as shown in Figs. 2(b) and 2(d), and Marangoni flow from the low- to the high-temperature side was induced. The inversion of the flow direction is reasonable considering the temperature dependence of the surface tension. As the temperature increases, the tension decreases and then increases ($\partial\gamma/\partial T < 0$ and $\partial\gamma/\partial T > 0$) in the N and I phases, respectively. The temperature dependence of the surface tension should result in flow
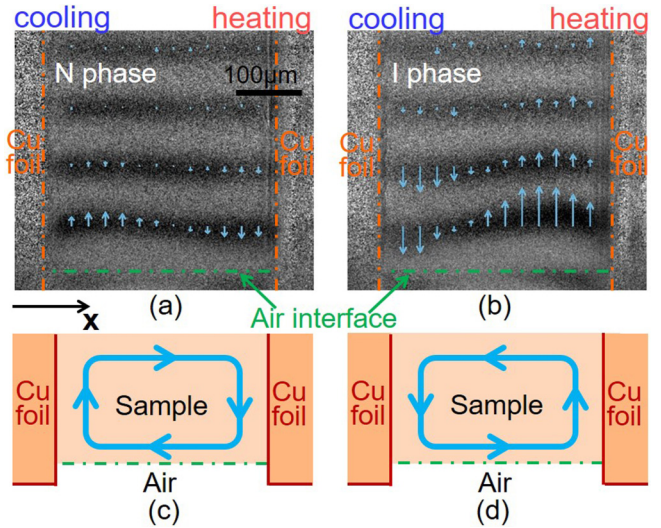

FIG. 2. Measurement results of the flow fields in the N and I phases. The green broken lines show the position of the air interface, and the black bar in (a) indicates 100 μm. The substrates were coated with Al1254, and the rubbing direction was along the x axis. The fluorescence microscope images obtained in the N and the I phases are shown in (a) and (b), respectively. Although straight-line regions were exposed to strong light illumination for photobleaching, the bleaching pattern showed a curved shape near the air interface owing to the existence of the flow. The aqua arrows in (a) and (b) indicate the y component of the flow velocity obtained by the measurement. The temperature at the middle position between the two copper foils was set to 36 °C in (a) and 47 °C in (b). The applied temperature gradient was 35 K/mm. From the flow field obtained in (a) and (b), the circulating flows illustrated in (c) and (d) were deduced, respectively.

generation toward the low- and high-temperature sides in the N and I phases, respectively.

The inversion of the direction of the Marangoni flow between the N and I phases was always observed and did not depend on the coating material of the cell substrates. However, the choice of the material strongly affected the flow field when the measurement was performed in the temperature region including the I-N transition point—that is, in the coexistence state of the I and N phases. The measurement results shown in Fig. 3 indicate that the flow toward the high-temperature side was induced in the air interface when the substrates were coated with Al1254 or CYTOP, while the flow was toward the low-temperature side in the case of JALS204 or DMOAP.

As described previously, the distribution of the y component of the flow velocity was measured by changing the temperature of the entire sample and the coating material of the cell substrate. Based on these measurement results, the flow velocity component along the x axis (defined as the direction of the temperature gradient) was estimated in the region near the air interface. Defining the x component of the velocity at the middle position between the two copper foil spacers as v_{x0}, its dependence on the temperature and the coating materials was obtained, as shown by the closed symbols in Fig. 4 (for more details, see Supplemental Material 2 [52]). In addition to Fig. 3, Fig. 4 clearly indicates that the flow direction depends on the coating materials near the
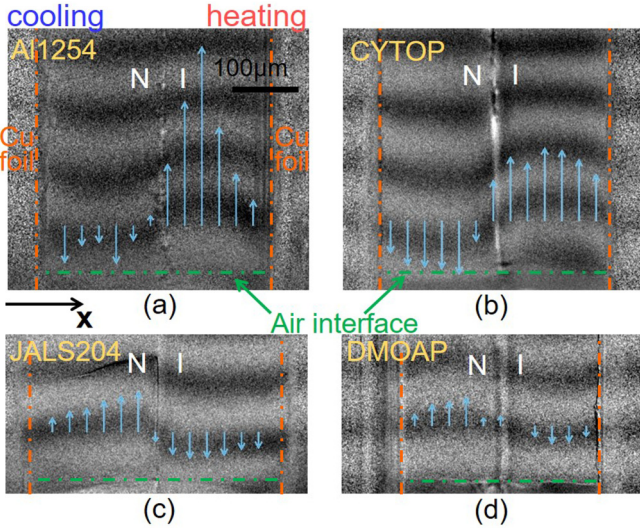
FIG. 3. Measurement results of the flow fields in the coexistence state of the I and the N phases. The green broken lines show the position of the air interface, and the black bar in (a) indicates 100 μm. The aqua arrows indicate the y component of the flow velocity obtained by the measurement. The coating material of the substrate is Al1254, CYTOP, JALS204, and DMOAP in (a)–(d), respectively. In (a), the rubbing direction was along the x axis. The temperature at the middle position between the two copper foils was set to 41 °C. The applied temperature gradient was 35, 29, 28, and 30 K/mm in (a)–(d), respectively.
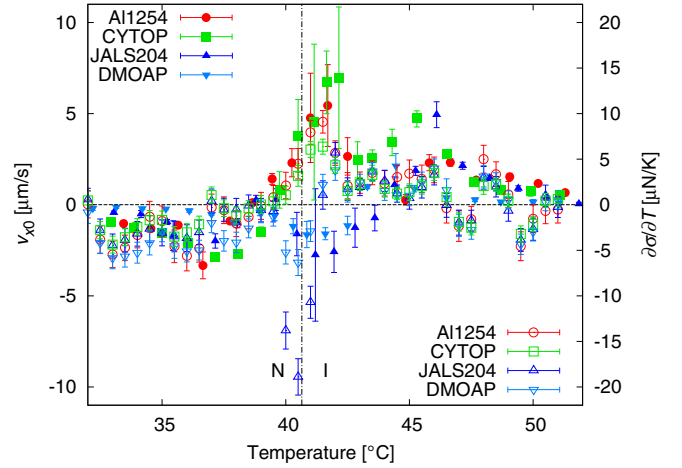

FIG. 4. Dependences of v_{x0} and $\partial\sigma/\partial T$ on temperature and coating materials of the substrates. The I-N phase transition temperature is shown by the chain line. Closed symbols show v_{x0} obtained by the flow-field measurement. In the measurement, the applied temperature gradient was 35, 29, 28, and 30 K/mm in Al1254, CYTOP, JALS204, and DMOAP, respectively, and v_{x0} is plotted with respect to the temperature in the middle position between the two copper foil spacers. Open symbols show $\partial\sigma/\partial T$ estimated by the measurement results of the temperature dependence of the surface tension γ and the contact angle θ_c. For the estimation, the mean average of γ and θ_c was used: in each temperature T, the measured values of γ and θ_c in the range from $T - 0.5$ °C to $T + 0.5$ °C were averaged. In addition, $\partial\gamma/\partial T$ and $\partial\theta_c/\partial T$ were obtained by fitting with linear functions ($\gamma = aT + \mathrm{const}$, $\theta_c = bT + \mathrm{const}$) for the measured values in the range from $T - 1.0$ °C to $T + 1.0$ °C. From the slope of the function (a and b) obtained in each T, the temperature dependencies of $\partial\gamma/\partial T$ and $\partial\theta_c/\partial T$ were estimated.

I-N phase transition point. This behavior cannot be explained only by the surface tension gradient, which should be uniquely determined under the given temperature field, because the surface tension is considered to be controlled by the interaction between the air and 7CB and not dependent on the choice of the coating material of the substrate. To explain why the flow direction depends on the coating material, it is necessary to consider another factor related to the interaction between the substrates and 7CB.

Here, it is considered that the Marangoni flow might be affected by the change in the contact angle between 7CB and the substrate—see θ_c in Fig. 1(b). When the angle θ_c changes, the area of the air interface also changes. This would affect the Marangoni convection with the prerequisite of the existence of the interface. The temperature dependence of θ_c strongly depended on the choice of the coating material of the substrate, as shown in the measurement results in Fig. 5. As the temperature decreased, a drastic decrease in θ_c was observed near the I-N transition point in the substrate coated with JALS204 or DMOAP, while the decrease was not significant in the case of Al1254 or CYTOP. This difference should be attributed to the dependence of the interface tension between 7CB and the substrate on the coating material, while in the present situation we cannot give an explanation based on microscopic molecular interactions for the difference of the interface tension (for more details, see Supplemental Material 3 [52]).

How the surface tension γ and contact angle θ_c affect the Marangoni flow was investigated using Onsager's variational principle [53,54]. According to this theory, the state

variation is determined by the minimization of the Rayleighian $\Re$, which is defined as the summation of the dissipation function W and the time variation of the free energy $\dot{F}_M$ given by the total differential ($\dot{F}_M = dF_M/dt$). Here, the suffix M was used considering that the energy variation could be attributed to the Marangoni effect. Here, $\Re$ at the air interface in the situation shown in Fig. 1 was estimated under the assumption that a unidirectional flow along the x axis exists with a velocity of V_x in the interface. It was also assumed that the temperature gradient is uniform along the x axis; thus, with the use of a constant α, the temperature T is described as $T = \alpha x + \mathrm{const}$. Here, considering that F_M does not explicitly depend on time and only the velocity component along the x axis exists in the flow field, $\Re$ at the air interface is estimated as

$$\Re = W + V_x \frac{\partial F_M}{\partial x} \sim \frac{\eta}{2}\left(\frac{V_x}{L}\right)^2 + V_x \alpha \frac{\partial F_M}{\partial T}, \quad (1)$$

where parameters L and η show the characteristic length and effective viscosity coefficient, respectively. They were not investigated in detail in this study.

In a cross-sectional view normal to the x axis, the length of the air interface is defined as l_s [see Fig. 1(b)]. Under the
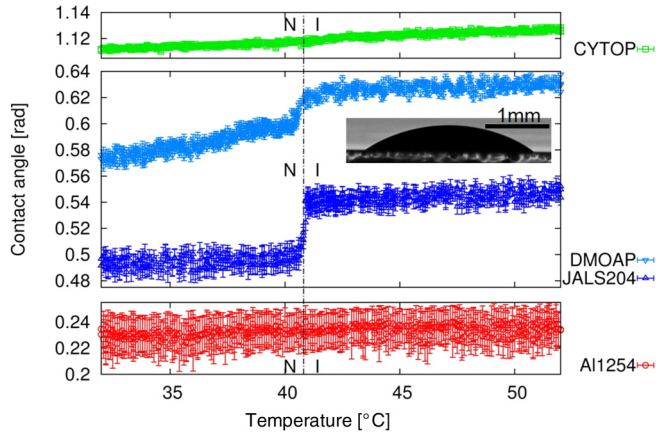
FIG. 5. Dependence of the contact angle on temperature and coating materials of the substrates. The I-N phase transition temperature is shown by the chain line. The contact angle was measured in a droplet on the cover glass coated with Al1254, CYTOP, JALS204, or DMOAP. The inset is a photograph of the droplet obtained in the measurement. The black bar indicates 1 mm. The temperature was set to 40 °C, and the coating material of the substrate was DMOAP.

assumption that the interface is arc shaped, l_s is expressed as

$$l_s = \frac{h(\pi - 2\theta_c)}{2\cos\theta_c}, \tag{2}$$

where h is the thickness of the sandwich cell. The free energy F_M should be proportional to γ and l_s (for more details, see Supplemental Material 4 [52] or Ref. [55]),

$$F_M \propto -\gamma l_s = -\sigma[\gamma(T), \theta_c(T)], \tag{3}$$

where σ is defined as the product of the temperature-dependent parameters γ and l_s. The flow velocity V_x is obtained by minimizing $\Re$ with respect to V_x ($\partial\Re/\partial V_x = 0$). Here, using Eqs. (1)–(3), one can obtain the following proportional relationship:

$$V_x \propto \frac{\partial\sigma}{\partial T}. \tag{4}$$

Using the measurement results of the temperature dependence of γ and θ_c in Supplemental Material 1 [52] and Fig. 5, $\partial\sigma/\partial T$ is estimated as described by the open symbols in Fig. 4. Near the I-N transition point (approximately 41 °C), the sign of $\partial\sigma/\partial T$ depends on the coating material: it is positive

for Al1254 or CYTOP and negative for JALS204 or DMOAP. This behavior is similar to that of the flow velocity obtained by the measurement (v_{x0}, closed symbols), which is consistent with Eq. (4).

As another possible reason for the dependence of the flow direction on the coating material, we should also discuss the flow induced by the capillary force, due to the gradient of the interface tension between 7CB and the substrate [2,12,55–58]. The variation of this interface tension γ_{LS} with respect to the temperature is comparable with that of the surface tension γ as estimated in Supplemental Material 1 and 3. Thus, it is possible to consider that the capillary force affects the flow field. However, in the present situation, how the capillary force results in the flow and whether such an effect works effectively remain to be elucidated (for more detail, see Supplemental Material 3 [52]). To address this problem, more detailed measurements of the flow and the temperature fields are necessary as a future task.

In this study, the Marangoni flow induced by the temperature gradient near the I-N transition point was observed using the fluorescence photobleaching method. In the air interface, flows toward the low- and high-temperature sides were observed in the N and I phases, respectively. The inversion of the flow direction is explained by the singularity in the temperature dependence of the surface tension γ near the I-N transition point: as the temperature increases, γ decreases in the N phase ($\partial\gamma/\partial T < 0$) and increases in the I phase ($\partial\gamma/\partial T > 0$). When the measurement of the flow field was performed in the I-N coexistence state, the flow direction depended on the coating material of the cell substrate. We considered that this dependence was attributed to the change in the area of the air interface near the I-N transition point. It was confirmed that the temperature dependence of the contact angle θ_c, which is directly related to the interface area, strongly depends on the coating material. Moreover, using the measurement results of γ and θ_c, the temperature dependence of the flow velocity was estimated based on Onsager's variational principle. This estimation is qualitatively consistent with the measurement results of the temperature dependence of the flow velocity. One can conclude that the Marangoni flow was driven by the area change of the air interface, in addition to the surface tension gradient.

[1] C. Borgnakke and R. E. Sonntag, *Fundamentals of Thermodynamics* (Wiley Global Education, New York, 2019).

[2] P.-G. de Gennes, F. Brochard-Wyart, and D. Quéré, *Capillarity and Wetting Phenomena: Drops, Bubbles, Pearls, Waves* (Springer, New York, 2003).

[3] D. Quéré, Annu. Rev. Fluid Mech. **45**, 197 (2013).

[4] A.-L. Biance, C. Clanet, and D. Quéré, Phys. Fluids. **15**, 1632 (2003).

[5] H. Linke, B. J. Alemán, L. D. Melling, M. J. Taormina, M. J. Francis, C. C. Dow-Hygelund, V. Narayanan, R. P. Taylor, and A. Stout, Phys. Rev. Lett. **96**, 154502 (2006).

[6] I. U. Vakarelski, N. A. Patankar, J. O. Marston, D. Y. C. Chan, and S. T. Thoroddsen, Nature (London) **489**, 274 (2012).

[7] T. Tran, H. J. J. Staat, A. Prosperetti, C. Sun, and D. Lohse, Phys. Rev. Lett. **108**, 036101 (2012).

[8] N. D. H. Dass, *The Principles of Thermodynamics* (CRC, Boca Raton, 2013).

[9] X. Xu and J. Luo, Appl. Phys. Lett. **91**, 124102 (2007).

[10] F. Girard, M. Antoni, and K. Sefiane, Langmuir **24**, 9207 (2008).

[11] Y. Kita, A. Askounis, M. Kohno, and Y. Takata, Appl. Phys. Lett. **109**, 171602 (2016).

[12] Y. Wen, P. Y. Kim, S. Shi, D. Wang, X. Man, M. Doi, and T. P. Russell, Soft Matter **15**, 2135 (2019).

[13] S. Shiri, S. Sinha, D. A. Baumgartner, and N. J. Cira, Phys. Rev. Lett. **127**, 024502 (2021).

[14] M. Gugliotti, J. Chem. Educ. **81**, 67 (2004).

[15] D. C. Venerus and D. N. Simavilla, Sci. Rep. **5**, 16162 (2015).

[16] A. Nikolov, D. Wasan, and J. Lee, Adv. Colloid Interface Sci. **256**, 94 (2018).

[17] V. X. Nguyen and K. J. Stebe, Phys. Rev. Lett. **88**, 164501 (2002).

[18] W. D. Ristenpart, P. G. Kim, C. Domingues, J. Wan, and H. A. Stone, Phys. Rev. Lett. **99**, 234502 (2007).

[19] R. Bhardwaj, X. Fang, and D. Attinger, New J. Phys. **11**, 075020 (2009).

[20] D. Brutin, B. Sobac, B. Loquet, and J. Sampol, J. Fluid Mech. **667**, 85 (2011).

[21] T. Still, P. J. Yunker, and A. G. Yodh, Langmuir **28**, 4984 (2012).

[22] H. Kim, F. Boulogne, E. Um, I. Jacobi, E. Button, and H. A. Stone, Phys. Rev. Lett. **116**, 124501 (2016).

[23] S. C. Hardy, J. Colloid Interface Sci. **69**, 157 (1979).

[24] S.-C. Tan, X.-H. Yang, H. Gui, Y.-J. Ding, L. Wang, B. Yuan, and J. Liu, Soft Matter **13**, 2309 (2017).

[25] E. Hendarto and Y. B. Gianchandani, J. Microelectromech. Syst. **23**, 494 (2014).

[26] P. Abolhosseini, M. Khosravi, B. Rostami, and M. Masoudi, J. Petrol. Sci. Eng. **164**, 196 (2018).

[27] K. Namura, K. Nakajima, K. Kimura, and M. Suzuki, Appl. Phys. Lett. **106**, 043101 (2015).

[28] H. Kawamura, K. Nishino, S. Matsumoto, and I. Ueno, J. Heat Transfer **134**, 031005 (2012).

[29] Q. Kang, D. Wu, L. Duan, L. Hu, J. Wang, P. Zhang, and W. Hu, J. Fluid Mech. **881**, 951 (2019).

[30] H. R. Holmes and K. F. Böhringer, Microsyst. Nanoeng. **1**, 15022 (2015).

[31] M. G. J. Gannon and T. E. Faber, Philosoph. Mag. A **37**, 117 (1978).

[32] V. A. Korjenevsky and M. G. Tomilin, Liq. Cryst. **15**, 643 (1993).

[33] B. Song and J. Springer, Mol. Cryst. Liq. Cryst. **307**, 69 (1997).

[34] Y. Martínez-Ratón, E. Velasco, A. M. Somoza, L. Mederos, and T. J. Sluckin, J. Chem. Phys. **108**, 2583 (1998).

[35] M. Tintaru, R. Moldovan, T. Beica, and S. Frunza, Liq. Cryst. **28**, 793 (2001).

[36] J.-W. Kim, H. Kim, M. Lee, and J. J. Magda, Langmuir **20**, 8110 (2004).

[37] L. S. Gomes and N. R. Demarquette, Mol. Cryst. Liq. Cryst. **437**, 181 (2005).

[38] C. Carboni, S. Al-Ruzaiqi, A. Al-Siyabi, S. Al-Harthi, A. K. George, and T. J. Sluckin, Mol. Cryst. Liq. Cryst. **494**, 114 (2008).

[39] K. Miyano, Phys. Rev. A **26**, 1820 (1982).

[40] H. Schüring, C. Thieme, and R. Stannarius, Liq. Cryst. **28**, 241 (2001).

[41] W. Urbach, F. Rondelez, P. Pieranski, and F. Rothen, J. Phys. (Paris) **38**, 1275 (1977).

[42] H. Choi and H. Takezoe, Soft Matter **12**, 481 (2016).

[43] J. Yoshioka and K. Fukao, Phys. Rev. E **99**, 022702 (2019).

[44] P. Oswald, J. Ignés-Mullol, and A. Dequidt, Soft Matter **15**, 2591 (2019).

[45] J. Yoshioka and F. Araoka, Sci. Rep. **10**, 17226 (2020).

[46] M. I. Godfrey and D. H. Van Winkle, Phys. Rev. E **54**, 3752 (1996).

[47] T. Trittel, K. Harth, C. Klopp, and R. Stannarius, Phys. Rev. Lett. **122**, 234501 (2019).

[48] R. Stannarius, T. Trittel, C. Klopp, A. Eremin, K. Harth, N. A. Clark, C. S. Park, and J. E. Maclennan, New, J. Phys. **21**, 063033 (2019).

[49] G. Lee, H.-C. Jeong, F. Araoka, K. Ishikawa, J. G. Lee, K.-T. Kang, M. Cepic, and H. Takezoe, Liq. Cryst. **37**, 883 (2010).

[50] J. Yoshioka, F. Ito, Y. Suzuki, H. Takahashi, H. Takizawa, and Y. Tabe, Soft Matter **10**, 5869 (2014).

[51] R. Stannarius and C. Cramer, Europhys. Lett. **42**, 43 (1998).

[52] See Supplemental Material at http://link.aps.org/supplemental/10.1103/PhysRevE.105.L012701 for experimental details of the measurement of surface tension, details about the estimation of interface tension between liquid crystal and substrate, and the definition of the free energy.

[53] M. Doi, J. Phys.: Condens. Matter **23**, 284118 (2011).

[54] M. Doi, *Soft Matter Physics* (Oxford University Press, New York, 2013).

[55] X. Man and M. Doi, Phys. Rev. Lett. **119**, 044502 (2017).

[56] S. Daniel and M. K. Chaudhury, Langmuir **18**, 3404 (2002).

[57] Y.-T. Tseng, F.-G. Tseng, Y.-F. Chen, and C.-C. Chieng, Sens. Actuators, A **114**, 292 (2004).

[58] Y. Hou, B. Xue, S. Guan, S. Feng, Z. Geng, X. Sui, J. Lu, L. Gao, and L. Jiang, NPG Asia Mater. **5**, e77 (2013).